

Accelerator Physics

Reported by Alan Jackson

For the majority of the ALS user community, 1997 could be characterized as a year of electron-beam stability. The previous year's efforts to master the intricacies of the transverse and longitudinal multibunch feedback systems, together with better control of the temperatures of the low-conductivity cooling water and storage-ring tunnel air, paid immense dividends in the stability of the beam during a fill. From this beginning, the Accelerator Physics Group embarked on the next level of stability—improving the undulator feed-forward system that ensures that the electron beam remains stable as the undulator gaps are changed at the user's request, fine tuning the electron orbit for best transmission of the photon beams to the experimental stations, and ensuring that the beam comes back to the same place, fill after fill, day after day.

To a large extent, as we describe below in the section on Storage Ring Setup, this goal has been achieved. However, since at the micron level we do not have a stable platform, we find it necessary to repeat our setup procedures at regular intervals—typically each week. Experimenters are certainly taking advantage of the enhanced stability by improving the resolution and/or reducing sampling times. In doing so, they are discovering small (but, to some experiments, significant) photon beam motion in the frequency range between 1 and 10 kHz. The Accelerator Physics Group is currently working with several user groups to identify, and hopefully eliminate, the sources of this motion.

Advances have also been made toward delivering higher quality beams for the “single-bunch” user community. During normal multibunch operation, we now offer a fill pattern known as the “camshaft fill.” In this pattern, we fill 288 sequential rf buckets to about 1.3 mA/bunch (to a total of 380 mA), plus a single bunch at 20 mA that sits inside a string of 40 empty rf buckets. While this is useful for some experiments, we still operate in two-bunch mode for the traditional time-of-flight spectroscopy experiments. These users require that the unpopulated buckets be truly empty. This has been achieved in the ALS (as at other facilities) by taking advantage of the differences in the betatron oscillation frequency between bunches with different charge densities. Transverse kickers, driven at the discrete frequency of the low-charge bunches, drive out the unwanted electrons without affecting electrons in the two highly populated bunches. In this way, the bunch purity has been improved from about 1:100 to better than 1:10000. Also, the currents that can be accumulated in a single bunch, limited by the transverse mode-coupling instability, have been increased from around 20 mA to 35 mA by the use of active feedback.

In addition to the work aimed directly at improving the quality of beams for users, the Accelerator Physics Group is engaged in a series of investigations to better understand the performance characteristics of the storage ring. As described below, these include investigations of beam lifetime, fast beam motion, reduction of the horizontal and vertical emittance, vacuum-vessel impedance, the fast beam-ion instability, and other non-linear beam dynamics in both transverse and longitudinal planes. Our group has also started work on a series of new initiatives:

- Designing a third-harmonic cavity system to lengthen the electron bunches (without increasing the energy spread of the beam), which will result in longer beam lifetimes.
- Meeting challenges associated with a new storage ring that is designed to have an emittance ten times smaller than that in the ALS (known internally as ALS-N).
- Developing methods for generating x rays in the 1-Å region of the spectrum with a pulse width of 100 fs FWHM.

ALS Storage Ring Setup

The operational parameters of the ALS can be varied over a wide range to meet the needs of the user. The ALS storage ring is capable of operating from 0.75 GeV to 1.9 GeV with almost any fill pattern utilizing from one to 328 rf buckets. The three most common modes of operation are 1.5-GeV multibunch, 1.9-GeV multibunch, and 1.9-GeV two-bunch (4 weeks/year). The multibunch pattern is typically 288 contiguous bunches with a gap for ion clearing. Often one of the empty rf buckets can be filled to high current to create pseudo-one-bunch operation (“camshaft” mode). Substantial progress was made in 1997 toward automating the setup; however, it is still a very machine-time-intensive activity. A full machine setup takes approximately eight hours, which is roughly one-third of the time allotted for accelerator physics studies.

General Storage Ring Setup

Reported by Greg Portmann

Many parameters have to be properly set in order for the storage ring to operate as designed. The storage-ring magnet lattice consists of 36 bends, 48 sextupoles, 72 quadrupoles, 4 skew quadrupoles, 94 horizontal correctors, and 70 vertical correctors. The other major systems include the rf system, the longitudinal-feedback system, and the transverse-feedback system. The main beam diagnostics are the 96 arc-sector beam-position monitors (BPMs), the 20 straight-section BPMs, the tune-measurement system, and the transverse and longitudinal beam-profile monitors (Beamline 3.1). To a large extent the setup and operation of the ALS storage ring has been automated. The setup process consists of accurately setting the parameters in the sequence shown in Figure 2-1. Some steps in the process require iteration.

Special attention was given to the orbit in 1997. A particular orbit, known as the “golden orbit,” was defined and then maintained all year. The criteria for defining the golden orbit are the following. First, the orbit is aligned to the center of the QF and QD magnet families. This minimizes the dispersion caused by going off-center in these magnets. Using the electron beam, the quadrupole centers can be measured to the 50- μm level. Second, in order to steer the photon beams down the beamlines, local orbit perturbations (typically displacements of about 100 μm and angles of 30 μrad) are added to the ideal orbit. Lastly, in the straight sections with small-gap vacuum chambers, the optimal orbit is the position that produces the maximum lifetime. Correcting back to the golden orbit every setup has essentially eliminated user requests for local orbit correction.

A simple local-steering feed-forward algorithm to compensate for field errors that change as the insertion device gaps are moved has proved to be extremely effective. The rms orbit distortion due to gap changes after generating a feed-forward table is typically $< 10 \mu\text{m}$. The difficulty with this method is that the feed-forward tables are strongly orbit dependent, so they need to be regenerated at every setup. Since each table takes about 15 minutes to generate, we are considering replacing this compensation method with one that relies on real-time closed-orbit feedback.

The setup and operation of the ALS storage ring are done using Matlab, a matrix-manipulation language. By connecting Matlab to the ALS control system, the large number of built-in functions for numerical methods in Matlab immediately become available for accelerator optimization. Automating the operation of the storage ring using this one application has improved orbit repeatability considerably by maintaining tight control of the many potential sources of error, such as magnet hysteresis. This has also reduced the time it takes to refill the storage ring and has removed some of the human errors that occasionally creep into day-to-day operation.

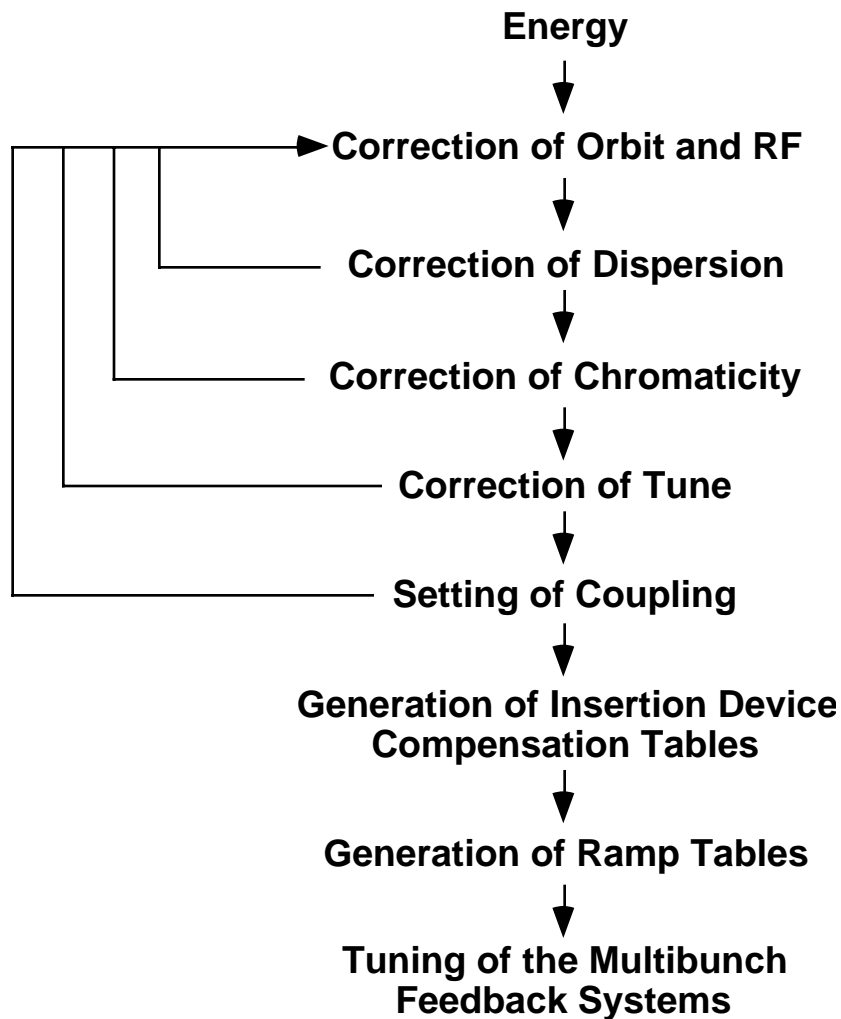


Figure 2-1. Canonical form of the storage ring setup process.

Two-Bunch Setup

Reported by John Byrd

Some synchrotron light users require single pulses of light spaced by at least several hundred nanoseconds. To satisfy this community, the ALS operates in a two-bunch mode about four weeks each year. In this mode, the ALS is filled with two bunches, diametrically opposite in the ring with 328-nanosecond separation. It is also important to the experiments that there be no parasite bunches in the ring. To optimize the machine performance, we are faced with the challenges of reaching high single-bunch current with reasonable lifetime while maintaining the purity of the two-bunch fill.

One limit to high current is a single-bunch effect known as the vertical mode-coupling instability (VMCI), driven by the broadband transverse impedance of the vacuum chamber. The effect is characterized by a sudden increase in vertical oscillations, resulting in a large increase in the effective vertical beam size and corresponding decrease in the brightness and stability of the beam. For the ALS, the threshold of this instability is presently about 16 mA/bunch. To achieve higher currents, we can damp the instability by increasing the lattice chromaticity (variation of betatron tune with electron momentum) from around 0.5 to 5. However, the higher chromaticity lowers the

energy acceptance, thereby increasing the loss of electrons from Touschek scattering, and lowering the lifetime. To avoid a lower lifetime, we have configured the vertical coupled-bunch feedback system to operate in a single bunch mode and tuned it to successfully reach > 30 mA/bunch, thereby doubling the current as compared to that high-chromaticity approach.

The second challenge in two-bunch operation is to achieve high bunch purity. The dominant mechanism through which parasite bunches are filled operates during the injection process. Imperfect bunching of the electron beam in the linac gun leads to a parasite bunch 8 nanoseconds from the main bunch with a charge as large as 1% of the main bunch. A more subtle mechanism, bunch-bunch diffusion, also comes into play (see the description in Figure 2-2). Rather than minimize the parasite filling during injection (which requires lowering the overall injection rate), we have developed a technique for cleaning out the parasite bunches immediately following injection. This technique takes advantage of the current-dependent vertical betatron frequency shift due to the transverse broadband impedance. At around 20 mA/bunch, the vertical betatron frequency has shifted about 15 kHz from the nominal frequency. This provides a selection mechanism for exciting only the low-current parasite bunches. We excite oscillations of the parasite bunches, utilizing the vertical kickers of the multibunch feedback system, to an amplitude large enough for them to be removed by a vertical scraper. Using this technique, we have reached purities (proportion of electrons in parasite bunches) of 10^{-4} and better.

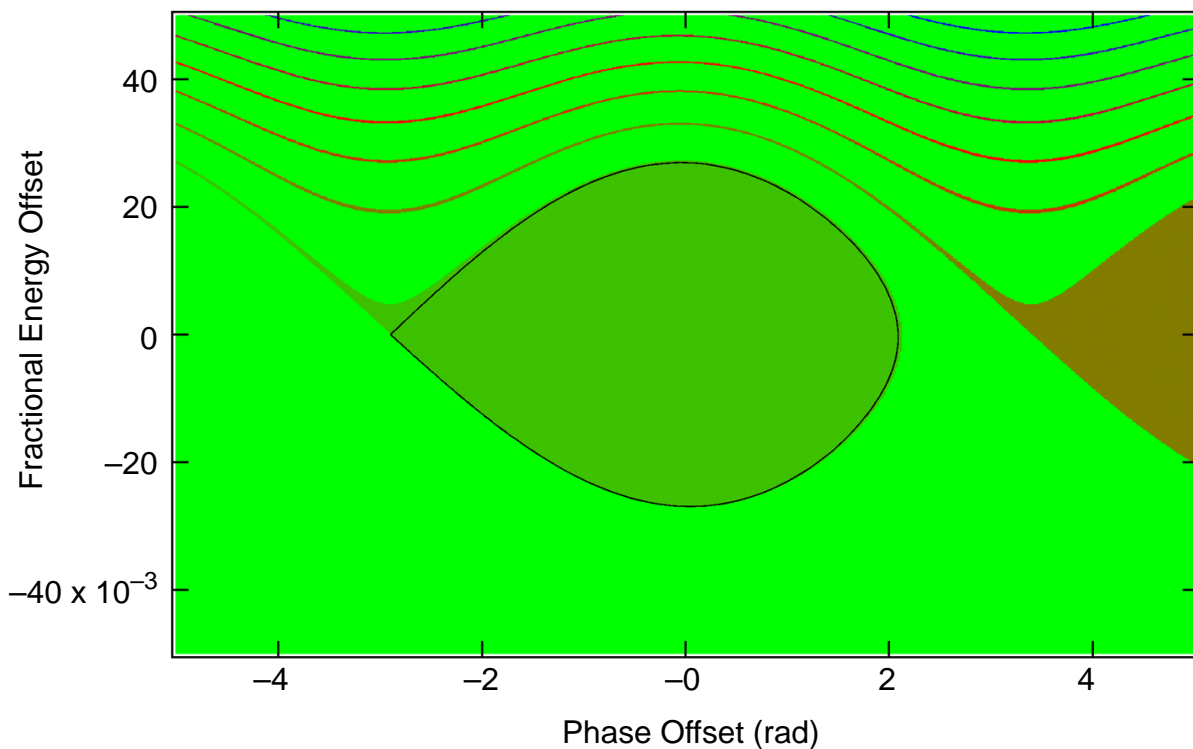


Figure 2- 2. Particle tracking with radiation damping. Ordinarily only the central dark-green region would be stable; electrons scattered out of it would be lost. With radiation damping, such electrons can be captured by the tail of the next bunch (brown, right side), where they are trapped in stable synchrotron orbits.

ALS Storage Ring Characterization

Reported by Greg Portmann

One of the more important user issues in 1997 was electron-beam stability. The stability requirement for the ALS has been steadily growing as each new beamline comes on line and as the more experienced users fine-tune their beamlines. Most ALS users are concerned with orbit motion below 100 Hz. However, beamlines like the infrared line required orbit stability (transverse and longitudinal) up to tens of kHz.

The electron-beam size in an ALS storage-ring straight section is approximately 250 μm horizontally and 16 μm vertically at 1.9 GeV. This small size poses difficult stability requirements for the storage-ring orbit—typically, ALS users would like orbit stability on the order of 10% of the beam size. Fortunately, the ALS storage ring inherently meets this requirement in the 1-Hz to 1000-Hz region. However, maintaining 25- μm horizontal and 1.6- μm vertical stability over the length of a fill (four hours) is very difficult without an orbit-feedback system.

Figure 2-3 shows the orbit and insertion-device gap motion over the length of a fill on March 26, 1998, a typical day. The “fast” orbit motion is only a few microns and the orbit “glitches” caused by errors in the feed-forward system are also only 1–5 μm , with one exception. At approximately 18.8 hours the horizontal orbit changed by about 40 μm because the insertion device in sector 5 (the wiggler) moved to a 14-mm gap. (The wiggler is usually kept at a fixed gap during user shifts to prevent this problem.) The dominant orbit distortions during this fill are slow temperature drifts, ± 20 μm horizontally and ± 10 μm vertically. Great effort has been spent stabilizing both the storage-ring air temperature and the LCW temperature. To a large extent, this effort has mitigated the orbit drift due to temperature; however, some days are better than others. To eliminate the problem, we are investigating a slow (but real-time) orbit-feedback system. Currently the limiting factor with orbit feedback is the positional stability and current dependence of the BPMs used for feedback.

In Figures 2-4 and 2-5 we take a closer look at the “fast” orbit stability of the storage ring electron beam. Figure 2-4 shows the power spectrum measured from 1 Hz to 300 Hz at insertion-device beam-position monitor (IDBPM) #2 in sector 12 during a 1.9-GeV user shift. The integral of the power spectrum, the rms displacement, amounts to 2.5 μm horizontally and 1.4 μm vertically. The shape of the power spectrum compares quite well with the shape of the ground-motion power spectrum calculated when including the structural bending modes of the ALS girders. Figure 2-5 shows a waterfall display of the power spectrum over eight hours. The change in rms displacement over the eight-hour period is very small; however, there is one anomalous peak that appears to migrate (usually in the 90-Hz to 300-Hz region). The cause of this peak is being investigated.

Very slow orbit motion (on a time scale of days) can cause misalignment of the photon beam through the photon-beamline optics. As shown in Figures 2-6 and 2-7, the day-to-day repeatability of the orbit can be quite good—remember that no orbit correction is done after the setup has been completed. The solid line in the plot shows the data from the upstream IDBPM, and the dashed line that of the downstream IDBPM, for each of the insertion device straight sections. Typically, the orbit stays within ± 150 μm horizontally and ± 50 μm vertically over a week’s time. However, the ALS orbit clearly has good days and bad days when considering stability over such long time periods. Table 2-2 summarizes orbit stability for different time durations. For frequencies below 1 Hz, it is very difficult to assign one number to the orbit stability when considering an entire year

because the day-to-day fluctuations can be reasonably large. The numbers in this table are conservative estimates.

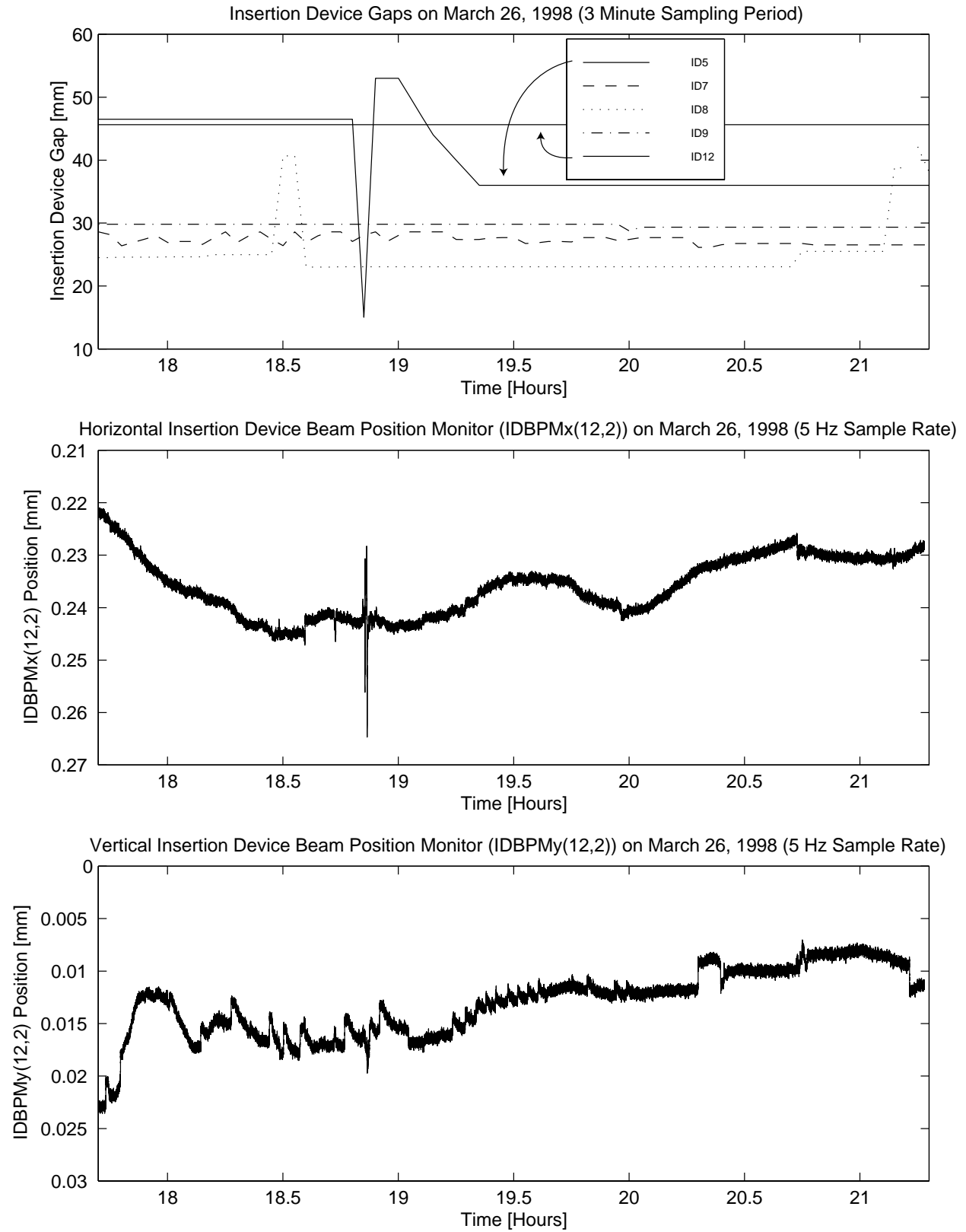


Figure 2-3. Plot of orbit motion over the course of a typical day shows the kind of long-term stability achievable with feedback.

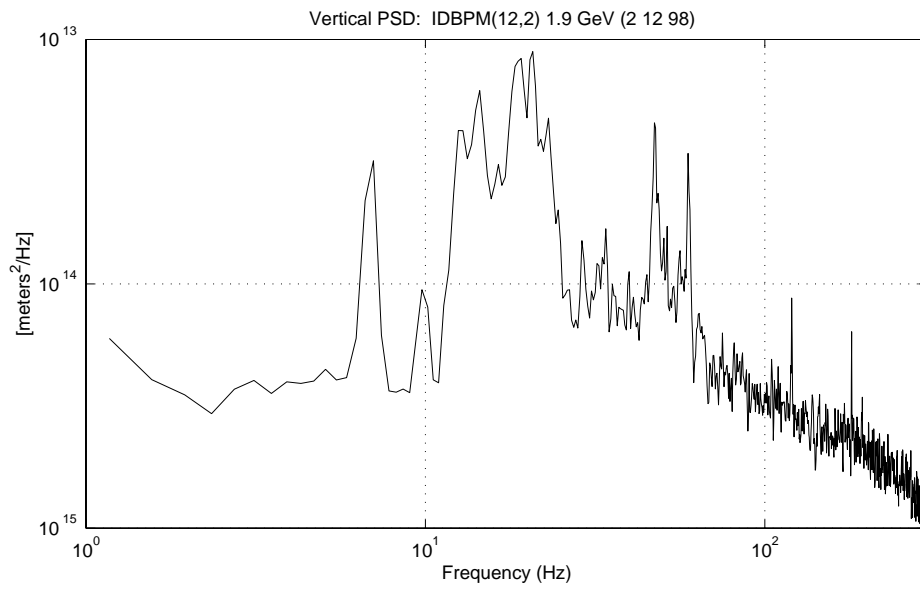
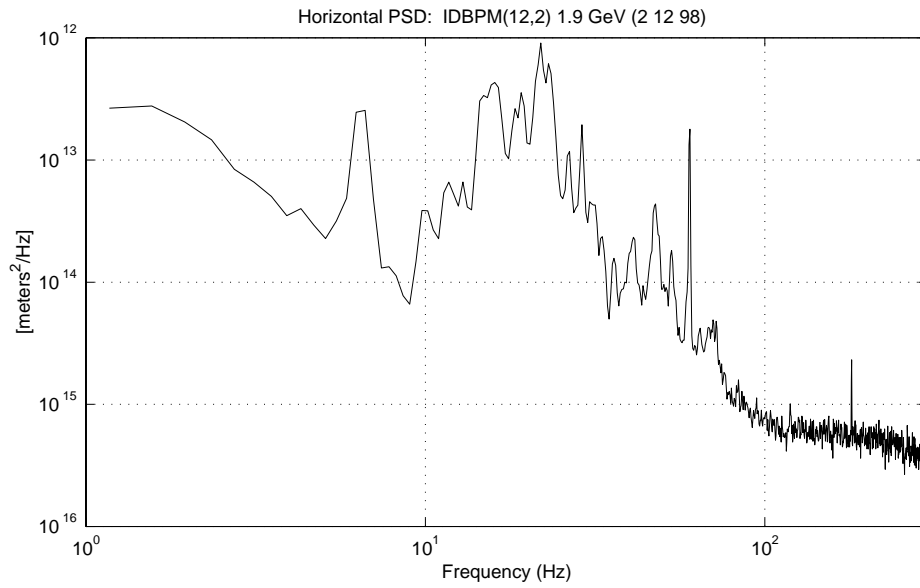


Figure 2-4. Power spectrum at insertion-device beam position monitor #2, sector 12.

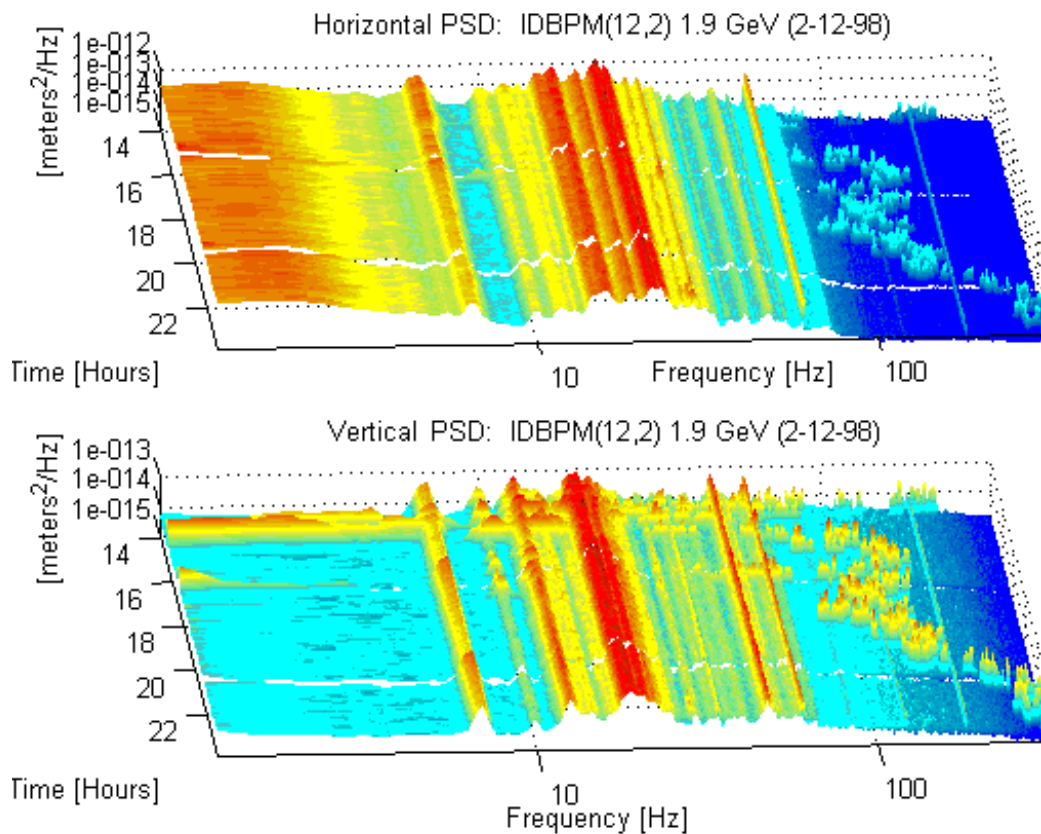
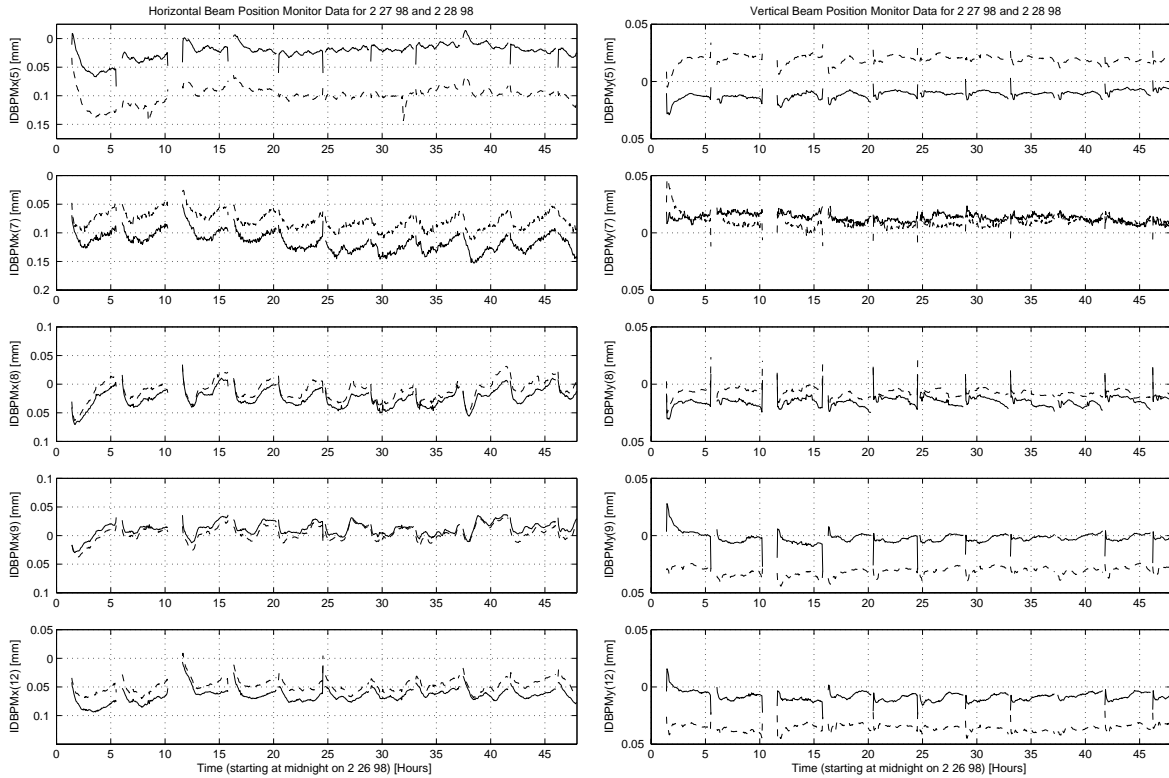


Figure 2-5. “Waterfall display” of the power spectrum shown in Figure 2-4 over an 8-hour period.

Table 2-2. ALS Storage Ring Stability.

“Frequency” Range	Magnitude ¹	Dominant Cause	Cure
Months	Difficult to measure	1. ALS floor setting 2. Seasonal temp. variation	Storage ring setup
Setup to setup repeatability	±200 μm Horizontally ±75 μm Vertically	1. Magnet hysteresis 2. Temperature fluctuations 3. Component heating between 1.5 and 1.9 GeV	Orbit correction
Days	±150 μm Horizontally ±50 μm Vertically	1. Temperature fluctuations	Orbit correction and/or improved temp. regulation
Length of a fill (4 Hours)	±50 μm Horizontally ±25 μm Vertically	1. Temperature fluctuations 2. Feed forward errors	Slow orbit feedback and/or improved temp. regulation
Minutes	5 to 10 μm	1. Feedforward errors	Slow orbit feedback
1 to 300 Hz	1 to 3 μm rms	1. Ground vibration	“Fast” orbit feedback
> 300 Hz	To be determined	To be determined	To be determined

¹ These are typical (and approximate) numbers that have been observed over the last year. The actual orbit fluctuations may vary depending on the day or new environmental conditions that arise. The orbit measurements were made at the straight-section beam-position monitors (IDBPMs).



Figures 2-6 (left) and 2-7. Orbit stability. Measurements of the beam position upstream (solid line) and downstream (dashed line) of insertion devices in the ALS storage ring show that the day-to-day reproducibility of the electron orbit can be quite good. Horizontal position is shown in Figure 2-6 at left, vertical position in Figure 2-7 at right.

Lifetime Measurements

Reported by Winfried Decking

The lifetime of the stored beam is one of the more important parameters of ALS storage-ring operation. For several reasons a long lifetime is desirable:

- The users have longer time spans in which to set up and run their experiments.
- A slower decay of the current leads to lower thermal variations in the vacuum chamber and beamline optics components.
- Higher average stored-beam current means, on average, more photons for the experimenters.

Several experiments were performed to obtain a better understanding of the effects that limit the lifetime in the ALS. The results of these measurements allowed us to differentiate between the various effects and pointed towards possible solutions to improve the lifetime.

The lifetime in an electron storage ring is usually determined by the following effects: the quantum lifetime (τ_q), elastic (τ_{el}) and inelastic scattering (τ_{inel}) of electrons by the residual gas atoms, scattering of electrons within the bunch (Touschek effect) (τ_{tou}), and trapping of charged particles in the beam potential (τ_{ion}). The total lifetime is given by:

$$\frac{1}{\tau_t} = \frac{1}{\tau_q} + \frac{1}{\tau_{inel}} + \frac{1}{\tau_{el}} + \frac{1}{\tau_{tau}} + \frac{1}{\tau_{ion}}$$

The functional dependencies of the lifetime effects on different machine parameters are as follows.

Quantum Lifetime:

$$\frac{1}{\tau_q} = \frac{1}{\tau_D} \frac{\Delta_{x,y,s}^2}{\sigma_{x,y,s}^2} \exp\left(-\frac{\Delta_{x,y,s}^2}{2\sigma_{x,y,s}^2}\right)$$

Elastic Scattering:

$$\frac{1}{\tau_{el}} = C_{el} \frac{1}{E^2} \left(\langle P \beta_x \rangle \frac{\beta_x}{\Delta_x^2} + \langle P \beta_y \rangle \frac{\beta_y}{\Delta_y^2} \right)$$

Inelastic Scattering:

$$\frac{1}{\tau_{inel}} = C_{inel} \langle P \rangle \ln\left(-\frac{1}{\Delta_s} + \frac{5}{8}\right)$$

Touschek Lifetime:

$$\frac{1}{\tau_{tou}} \approx C_{tou} \frac{1}{E^3} \frac{I_{bunch}}{\text{Volume} \Delta_s^2} f(\Delta_s \sigma_x', E)$$

In these equations, $\Delta_{x,y}$ is the transverse aperture, $\beta_{x,y}$ the β -functions, and $\sigma_{x,y}$ the beam size at the position of the aperture. σ_s is the width of the longitudinal particle distribution, and Δ_s the longitudinal acceptance of the storage ring. The longitudinal acceptance can be determined by the size of the rf bucket or by the dynamic acceptance.

The damping time τ_D is a known function of the storage ring parameters (between 13 and 17 ms at the ALS). C_{el} and C_{inel} depend on the constitution of the residual gas. Assuming that the gas consists of 100% nitrogen, $C_{el} = 38.88 \text{ GeV}^2/\text{mbar h}$, and $C_{inel} = 4.2 \times 10^6/\text{mbar h}$ at 300 K. We will refer the gas pressure P to this “standard” atmosphere. $\langle P \rangle$ is the average gas pressure around the ring and $\langle P \beta_{x,y} \rangle$ is the average product of the local pressures and β -functions around the ring. The gas pressure (and distribution) varies with total beam current because of desorption effects:

$$\langle P \rangle = \langle P_0 \rangle + \frac{dP}{dI} I_{total}$$

where dP/dI is the gas desorption coefficient and I_{total} is the total beam current.

The quantum lifetime is only important for transverse apertures smaller than $\approx 6 \sigma$, which corresponds to 1.2 mm horizontally and 0.08 mm vertically (for standard 1.5-GeV operating conditions) at the position of the scraper.

When electrons scatter within a bunch, they may transfer enough momentum from transverse oscillations into longitudinal motion, to be outside the momentum acceptance of the storage ring. This effect is proportional to the electron density within a bunch. Assuming a flat beam, so that the main contribution to the velocity spread comes from horizontal motion, gives the Touschek lifetime shown above. In this equation, I_{bunch} is the bunch current and Volume is the bunch volume. The bunch volume varies around the ring, thus the Touschek lifetime has to be averaged around the ring. The function f varies slowly with Δ_s and σ_x' . For this investigation we only use the fact that τ_{tou} is inversely proportional to the bunch current.

Recent work at the ALS extended the classical one-dimensional theory to the general three-dimensional case, taking into account the velocity spread in all three dimensions. For standard ALS operating conditions, the new theory agrees with the classical one to within 10%.

Transverse Scraper Measurements

The quantum lifetime and the elastic-scattering lifetime directly depend on the available transverse aperture, which can be varied with beam scrapers. The dependency of the lifetime on the scraper position reveals information about the gas pressure at the beam position, the transverse beam sizes, and the limiting transverse aperture.

The Touschek and inelastic scattering lifetime depend only indirectly on the scraper position. Inserting a scraper can also reduce the longitudinal acceptance of a storage ring, which is the defining aperture for these lifetime effects. The scraper measurements were thus done at a low bunch current. This minimizes the contribution from the Touschek effect.

Results of several measurements with horizontal and vertical scrapers are shown in Figure 2-8. The measured lifetime as function of horizontal scraper position was fitted to the following curve:

$$\frac{1}{\tau}(\Delta_x) = \begin{cases} \text{const.} & \text{if } \Delta_x > A_x \\ \frac{1}{\tau_{\text{tou+inel}}} + C_{\text{el}} \frac{1}{E^2} \langle P \rangle \left(\langle \beta_x \rangle \frac{\beta_x}{\Delta_x^2} + \langle \beta_y \rangle \frac{\langle \beta_y \rangle}{\Delta_y^2} \right) & \text{if } \Delta_x < A_x \end{cases}$$

where $A_{x,y}$ is the real aperture of the storage ring. Exchanging x and y allows us to fit the lifetime for the vertical scraper position. As the real aperture of the storage ring is not known, this fitting procedure is done iteratively to determine the apertures that best fit the measurements.

The average pressure around the ring was determined to be $\langle P \rangle(5 \text{ mA}) \approx 5 \times 10^{-10}$ mbar from the horizontal-scraper measurement and $\langle P \rangle(5 \text{ mA}) \approx 2 \times 10^{-10}$ from the vertical-scraper measurements. This discrepancy could be due to higher pressure at locations where the ratio of the horizontal to the vertical β -functions is 5/2, as for example in the straight sections. Assuming these β -functions, the average pressure is $\langle P \rangle(5 \text{ mA}) \approx 3 \times 10^{-10}$ mbar.

We define the acceptance $A_{x,y}$ of the ALS as the point where the lifetime stays constant with changing scraper positions. The horizontal acceptance is thus $A_x \approx 10 \text{ mm}$ to 12 mm , which is much smaller than what we expect from tracking calculations. The vertical acceptance is $A_x \approx 3.5 \text{ mm}$ to 4 mm , which is in agreement with the free aperture of the narrow-gap chambers.

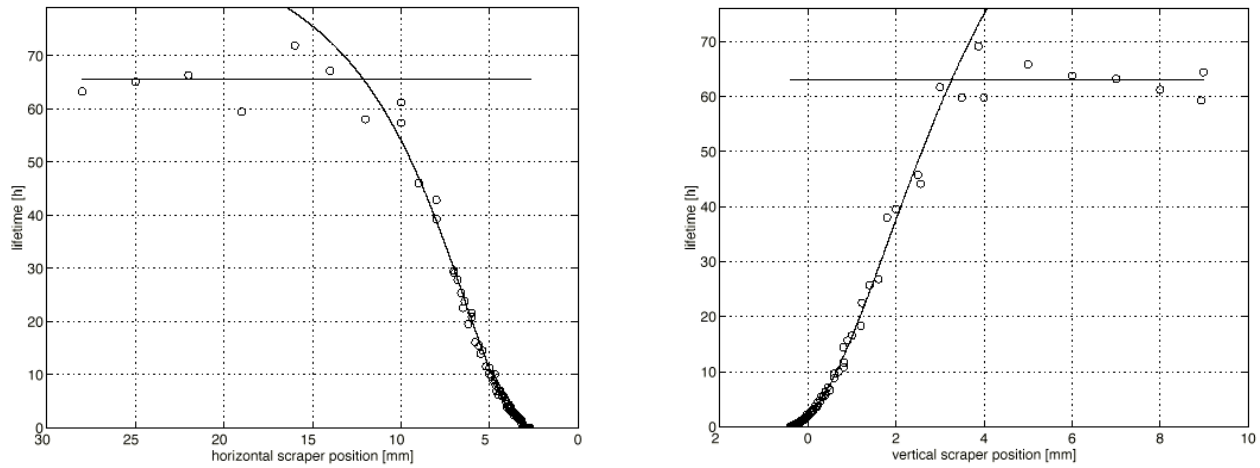


Figure 2-8. Lifetime as a function of the horizontal (left) and vertical (right) scraper position. The storage-ring parameters were beam current 5 mA in 288 bunches, beam energy 1.5 GeV, and multibunch feedback off.

This information allows one to calculate the contributions of the different lifetime effects to the total lifetime at 5 mA in 288 bunches. As the current per bunch is very small, the Touschek lifetime is very large. A measurement of the lifetime at the same total current but with varying bunch currents (i.e. number of bunches) is shown in Figure 2-9.

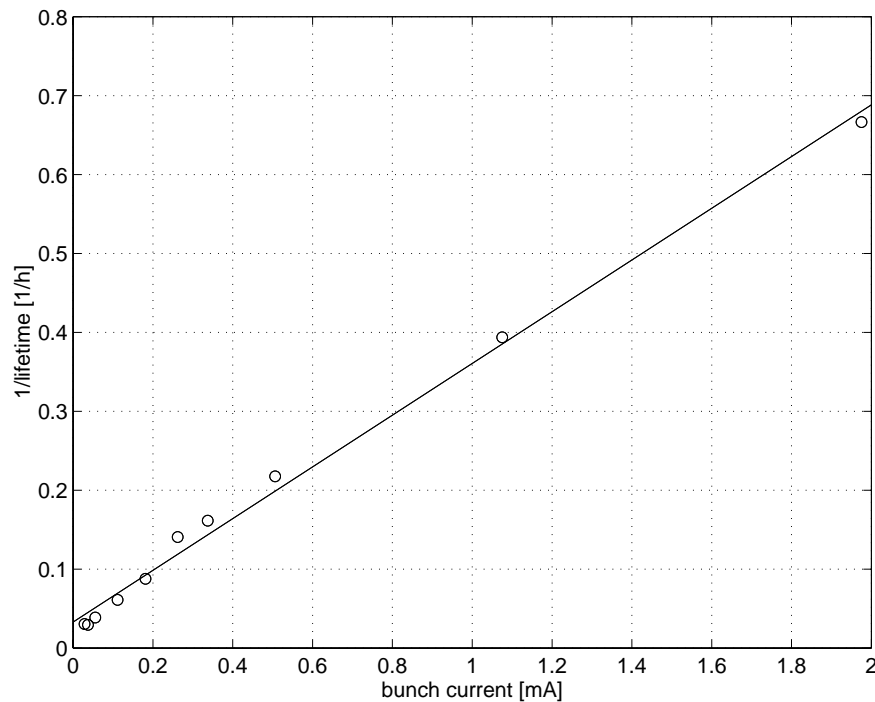


Figure 2-9. Inverse life-time versus bunch current. The total current is held constant in this measurement.

As the gas pressure does not change in this experiment, the slope of the curve gives the change of the Touschek lifetime with bunch current at 1.5 GeV:

$$\frac{1}{\tau_{\text{tou}}} = 0.33 \left[\frac{1}{\text{h} \cdot \text{mA}} \right] I_{\text{bunch}}$$

Remember, the Touschek lifetime changes with the bunch volume, thus any variations of this parameter will change the coefficient given above.

Table 2-3 summarizes the different contributions to the total beam lifetime for 1.5 GeV and 288 bunches (i.e., standard operating conditions). We assumed that the gas is distributed more uniformly for the 400 mA case, as the gas desorption probably takes place in the arcs rather than in the straight sections.

Table 2-3. Contributions of the lifetime limiting effects to the total lifetime at 5 mA and 400 mA in 1.5 GeV operation.

	5 mA	400 mA
quantum lifetime τ_q	∞	∞
elastic scattering lifetime τ_{el}	85 hours	>18 hours
inelastic lifetime τ_{inel}	265 hours	>55 hours
Touschek lifetime τ_{tou}	≈ 200 hours	2.2 hours
total lifetime τ_t	50 hours	>1.9 hours

Table 2-3 shows that, at standard operating conditions, the Touschek lifetime dominates the total beam lifetime. But even with a fully coupled beam, the lifetime would not exceed 16 hours, which is in agreement with measurements showing a 15-hour lifetime under these conditions.

As the Touschek lifetime is the limiting effect for ALS operations, several options are available to increase it. The most obvious is to increase the bunch volume, which is currently done by increasing the vertical beam size with the help of skew quadrupoles. This leads to a reduction in the brightness. A better way is to elongate the beam with the help of a third-harmonic cavity, which we plan to install in the near future.

Another possibility is to increase the longitudinal acceptance, Δ_s . At a beam energy of 1.5 GeV, the measured longitudinal acceptance is smaller than we expect. The reason for this is currently under investigation. However, at a beam energy of 1.9 GeV, the momentum acceptance is limited by the available rf power. Plans are under way to increase the rf power.

Lower Beam Emittances

Reported by Alan Jackson

Recently it has been recognized that the bend-magnet radiation from the center bends of the ALS triple-bend achromat lattice is extremely bright, primarily because of the small beam sizes at these source points. The beam sizes can be made smaller yet by reducing the horizontal and vertical beam emittances, and/or reducing the β -functions at the source points, and/or reducing the dispersion function at the source points. In practice, all three conditions tend to go together, as we see from the equation below, the emittance ϵ is a function of the lattice functions (β , α , η , η') in the bend magnets.

$$\epsilon \propto \int_{\text{dipoles}} \left(\gamma_x \eta_x^2 + 2\alpha_x \eta_x \eta_x' + \beta_x \eta_x'^2 \right) ds$$

The values of these functions can be manipulated by adding quadrupoles in the achromatic arcs or by permitting the dispersion function to be non-zero in the long straight sections. We are currently simulating these possibilities using the lattice design and analysis code TRACY-V.

In the upper panel of Figure 2-10, we show an example in which the natural (zero-beam limit) emittance is reduced from 3.6 nm-rad to 2.1 nm-rad simply by increasing the strengths of the QFA family of quadrupole magnets (the so-called “momentum quads”). Analysis of the dynamic aperture (Figure 2-10, lower panel), with the usual complement of alignment-error terms included, suggested that there is sufficient aperture for injection and acceptable beam lifetime.

Four hours of accelerator beam time were allocated for a “trial run” to check the predictions of the simulation (e.g., the tune change as QFA is varied), and in this time we were able to stack beam at the new working point—a true testament to the predictive capabilities of TRACY-V. A measurement of the beam-size at the diagnostic beamline (Beamline 3.1), confirmed that the emittance was reduced to the expected value (within a measurement error of $\pm 20\%$). It is unlikely that this new working point will be offered to users any time soon, since the beam lifetime (through Touschek scattering) suffers significantly. However, it is an operating mode that may well become desirable after the lifetime is enhanced by implementation of the third-harmonic cavity system.

Vertical beam sizes are determined mainly through field errors in the lattice magnets that result in coupling of transverse energy from the horizontal plane to the vertical plane (a process known as betatron oscillation coupling) and in generating vertical dispersion in the bend magnets. We are now trying to reduce the coupling and vertical dispersion using skew quadrupoles and vertical correctors.

Observation and Characterization of the Fast Beam-Ion Instability

Reported by John Byrd

A new regime of ion trapping has been predicted, first described by Raubenheimer and Zimmerman [*Phys. Rev. E* **52**, 5487-5498 (1995)], where ions generated and trapped during the passage of a *single* train lead to a fast instability. In this case, a gap in the bunch train does not help because the instability develops over a single passage of the beam. As a bunch train passes through the storage ring, it ionizes residual gas. A small oscillation of the electron beam drives oscillations of the ions, which in turn drive subsequent bunches in the electron beam. Through this amplification mechanism, small oscillations at the head of the bunch train drive large oscillations at the tail. In many future rings, this transient instability is predicted to have very fast growth rates, much faster than the damping rates of existing and proposed transverse-feedback systems, and thus is a potential limitation.

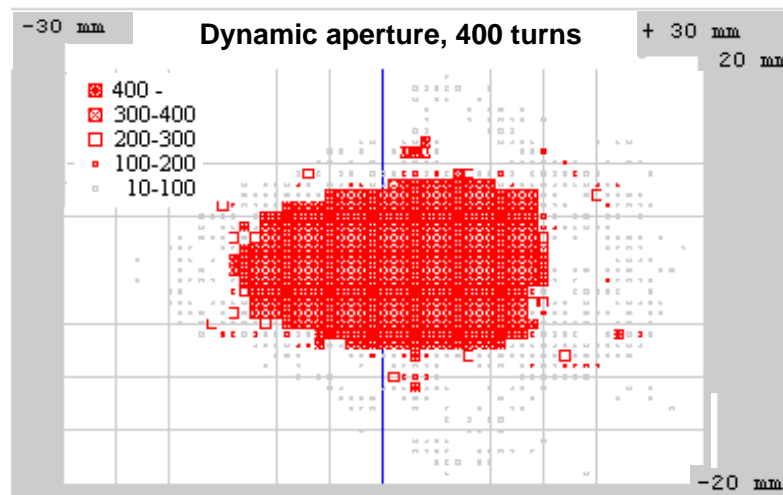
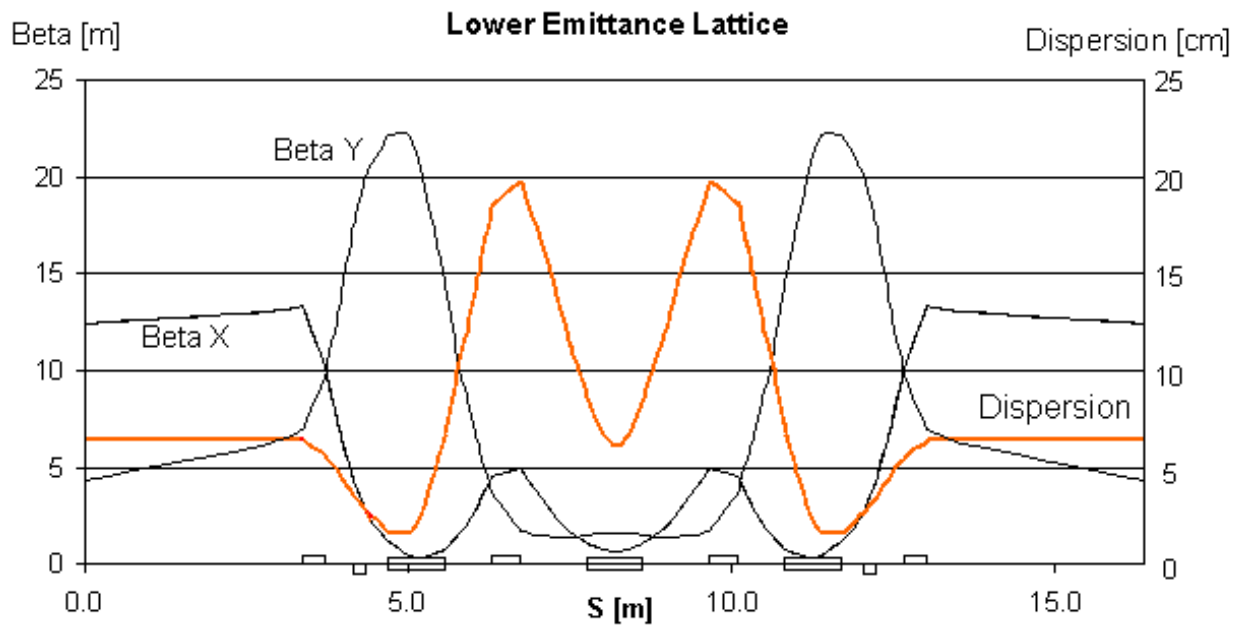


Figure 2-10. TRACY-V plots of how emittance could be reduced with adequate dynamic aperture simply by increasing the strengths of the QFA or “momentum” quadrupoles.

A collaboration between the ALS Accelerator Physics Group and physicists from Stanford Linear Accelerator Center was the first to observe and characterize this potentially important instability [J. M. Byrd, A. Chao, S. Heifets, M. Minty, T. O. Raubenheimer, J. Seeman, G. Stupakov, J. Thomson, F. Zimmermann, *Phys. Rev. Lett.* **79**, 79-82 (1997)]. Since the initial experiments, further measurements have tested methods proposed to cure the instability, such as filling the storage ring with short bunch trains and gaps larger than the ion wavelength. The short length of the bunch train allows very little time for the amplification mechanism to occur, and the gap allows collected ions to drift away. Comparison of the beam stability with a continuous bunch train and a series of short trains indicated that this technique is successful in avoiding the fast instability.

Single-Bunch Instabilities

Reported by John Byrd

Single-bunch instabilities are driven by short-range wakefields, which typically decay over the length of the bunch. Longitudinal effects include distortion of the longitudinal bunch distribution and increase of the energy spread. Transverse effects include the mode-coupling instability in the vertical direction which limits the single-bunch current to about 16 mA (at zero chromaticity.) We have begun an effort (in collaboration with M. Migliorati, University of Rome-La Sapienza) to characterize the longitudinal short-range wakefields by measurements of the bunch length and energy spread as a function of single bunch current. Shown below (Figures 2-11 and 2-12) are examples of such measurements at a beam energy of 1.5 GeV. The longitudinal bunch profile was measured using a streak camera on the diagnostic beamline (Beamline 3.1). The lengthening of the bunch is evident, as well as a distortion of the shape where the front of the bunch becomes steeper than the rear.

Preliminary analysis of the measurements indicates that the measurements are consistent with a simple resistive/inductive impedance model of the ring with a resistance of 580 ohms and an inductance of 80 nanohenries. This model is currently being refined and compared with numerical computation of the wakefield, as well as computer simulations of the beam dynamics.

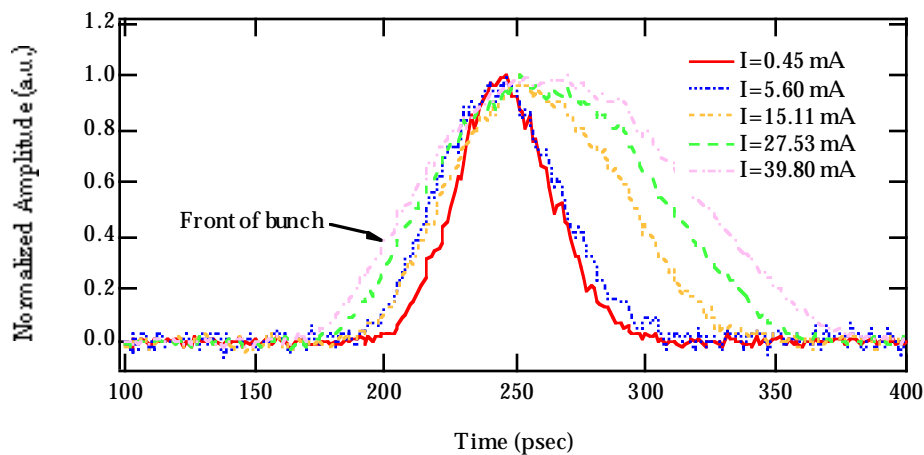


Figure 2-11. Bunch shape, measured as a function of bunch current.

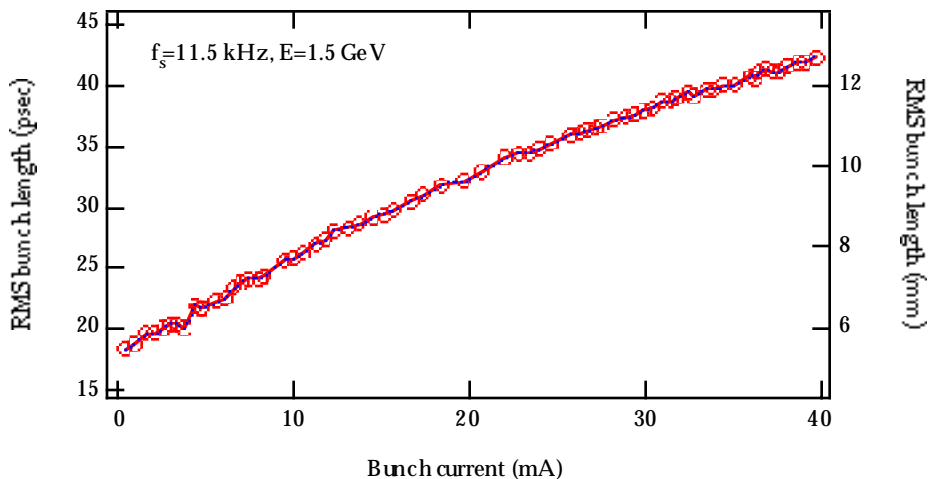


Figure 2-12. Bunch length as a function of bunch current. Imagine each of the circles in this figure being expanded to a shape distribution like the one in Figure 2-11.

Longitudinal Beam-Transfer-Function Diagnostics in an Electron Storage Ring

Reported by John Byrd

Beam-transfer-function (BTF) diagnostics are used in almost all storage rings for measuring the betatron and synchrotron frequencies. In the simplest case, a swept frequency drive excites either betatron or synchrotron oscillations while a beam signal is observed on a spectrum analyzer. In other applications, BTF techniques have been used for measuring beam impedance and feedback-loop stability. In recent studies at the ALS, we have used the BTF technique to measure the distribution of synchrotron frequencies within a single bunch at low beam-current modulation [J.M. Byrd, *Particle Accelerators* **57** (No. 3), 159 (1997)]. By taking advantage of the Gaussian distribution in the energy spread within the bunch, resulting from the quantum nature of the emission of synchrotron radiation and the sinusoidal rf voltage, we can use these measurements to derive a precise measure of the nominal synchrotron frequency, the longitudinal radiation damping rate, and the bunch length.

Although these parameters can be measured using other techniques, the BTF method has the advantage of being relatively simple and inexpensive, as it typically uses equipment that is already available in the control room. The BTF technique can potentially be used to study the effects of short-range wakefields and the longitudinal beam dynamics of more complicated situations, such as double-rf systems and low-momentum compaction. Shown below (Figure 2-13) is a measurement of the longitudinal BTF of the storage ring, along with a fit using the theoretical parameters of the BTF. For ALS conditions, the width of the synchrotron resonance is determined by a combination of the spread in synchrotron frequencies within the bunch and the width of the response of individual electrons due to radiation damping.

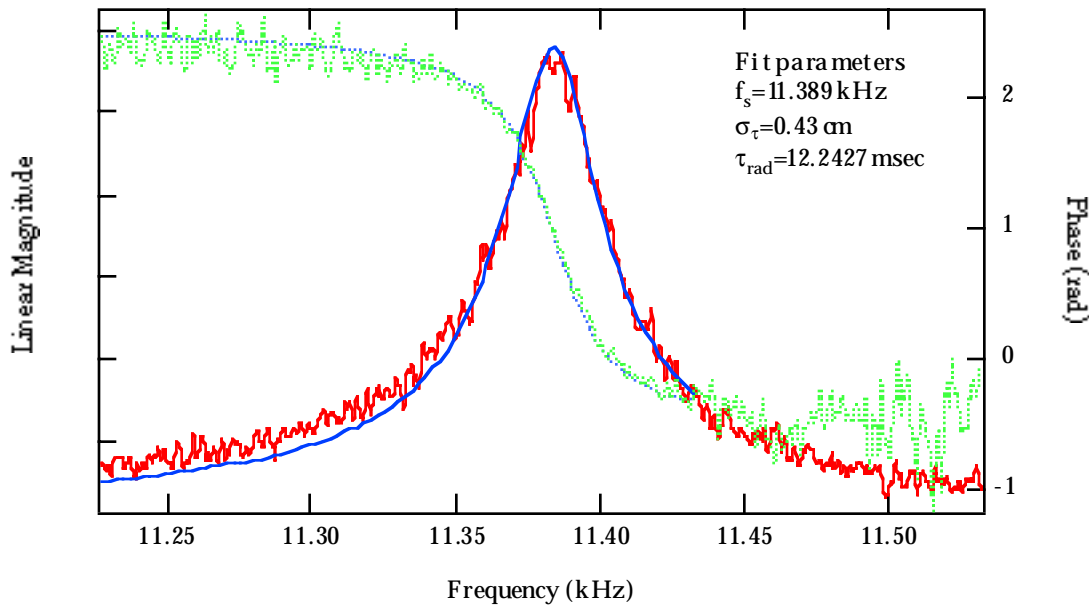


Figure 2-13. A measurement of the longitudinal BTF of the storage ring, along with a fit using the theoretical parameters of the BTF.

Nonlinear Longitudinal Dynamics with Phase Modulation

Reported by John Byrd

The ALS has suffered from longitudinal and transverse coupled-bunch instabilities since it was commissioned. In the case of longitudinal instabilities, the beam oscillations grow to a certain level and stop, probably due to a nonlinear saturation mechanism. As a first step in understanding this saturation mechanism, as well as nonlinear dynamics in general, we have performed a series of experiments to study nonlinear synchrotron oscillations in the presence of strong phase modulation [J. M. Byrd, W.-H. Cheng and F. Zimmermann, *Phys. Rev. E* **48**, 4678 (1998)].

We studied this phenomenon using a dual-scan streak camera in synchroscan mode. This allowed us to observe the time evolution of the longitudinal distribution of a single bunch as the modulation frequency is swept through the synchrotron frequency. Shown below (Figure 2-14) is an example of the longitudinal distribution for three modulation frequencies. The vertical axis is time with respect to a synchronous bunch (i.e., a bunch not executing synchrotron oscillations), where positive displacement indicates early arrival. The horizontal axis represents the relatively slow sweep time of the streak camera. For these images, the horizontal time scale is about 530 turns. The darker area in the image represents higher intensity. The sinusoidal pattern of the distribution is due to the phase modulations (the nominal RMS bunch length is 15 ps to 20 ps.) At this level of excitation, the bunch has oscillation amplitude of about 100 ps to 300 ps peak-to-peak. At the bifurcation frequency, the bunch appears to split into two separate beamlets, oscillating with different amplitudes and out of phase by 180 degrees. The charge in the second beamlet increases while the first decreases. Above the bifurcation frequency, the original beamlet disappears and only the second remains. The time at which the second beamlet appears depends on the modulation sweep rate and the bunch current. We observe similar effects for downward sweeps of the modulation frequency, which are also dependent on sweep rate and bunch current.

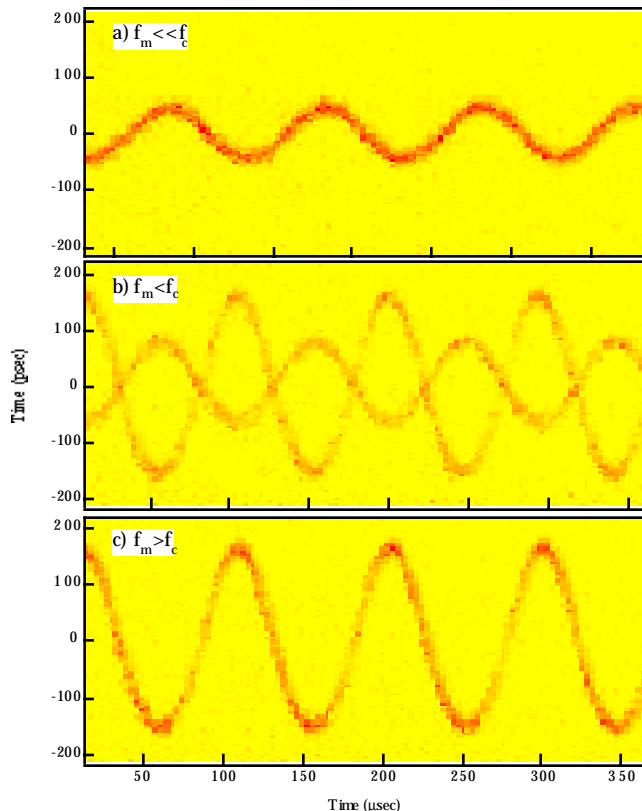


Figure 2-14. Time evolution of the longitudinal distribution of a single bunch at modulation frequencies much less than (top), slightly less than, and slightly greater than the synchrotron frequency.